Atmos. Chem. Phys. Discuss., 13, 3817–3858, 2013
www.atmos-chem-phys-discuss.net/13/3817/2013/
doi:10.5194/acpd-13-3817-2013

Atmospheric Chemistry and Physics Discussions

Modeling the present and future impact of aviation on climate: an AOGCM approach with online coupled chemistry

P. Huszar[1,4], H. Teyssèdre[1], D. Cariolle[1,2], D. J. L. Olivié[1,3], M. Michou[1], D. Saint-Martin[1], S. Senesi[1], A. Voldoire[1], D. Salas[1], A. Alias[1], F. Karcher[1], P. Ricaud[1], and T. Halenka[4]

[1]GAME/CNRM, Météo France, UMR3589, CNRS, Toulouse, France
[2]Centre Europeén de Recherche et de Formation Avancée en Calcul Scientifique, CERFACS/CNRS, Toulouse, France
[3]University of Oslo and CICERO, Oslo, Norway
[4]Department of Meteorology and Environment Protection, Faculty of Mathematics and Physics, Charles University, Prague, V Holešovičkách 2, Prague 8, 180 00, Czech Republic

Received: 11 January 2013 – Accepted: 1 February 2013 – Published: 11 February 2013

Correspondence to: P. Huszar (peter.huszar@mff.cuni.cz)

Published by Copernicus Publications on behalf of the European Geosciences Union.

Abstract

This work assesses the impact of emissions from global aviation on climate, while focus is given on the temperature response. Our work is among the first that use an Atmosphere Ocean General Circulation Model (AOGCM) online coupled with stratospheric chemistry and the chemistry of mid-troposphere relevant for aviation emissions. Compared to previous studies where either the chemical effects of aviation emissions were investigated using global chemistry transport models or the climate impact of aviation was under focus implementing prescribed perturbation fields or simplified chemistry schemes, our study uses emissions as inputs and provides the climate response as output. The model we use is the Météo-France CNRM-CM5.1 earth system model extended with the REPROBUS stratospheric scheme. The timehorizon of our interest is 1940–2100 assuming the A1B SRES scenario. We investigate the present and future impact of the most relevant aviation emissions (CO_2, NO_x, contrail and contrail induced cirrus – CIC) as well as the impact of the non-CO_2 emissions and the "Total" aviation impact. Aviation produced aerosol is not considered in the study.

The general conclusion is that the aviation emissions result in a less pronounced climate signal than previous studies suggest. Moreover this signal is more unique at higher altitudes (above the mid-troposphere) than near the surface.

The global averaged near surface CO_2 impact reaches around 0.1 °C by the end of the 21st century and can be even negative in the middle of the century. The non-CO_2 impact remains positive during the whole 21st century reaching 0.2 °C in its second half. A similar warming is calculated for the CIC effect. The NO_x emissions impact is almost negligible in our simulations, as the aviation induced ozone production was small in the model's chemical scheme. As a consequence the non-CO_2 signal is very similar to the CIC signal. The seasonal analysis showed that the strongest warming due to aviation is modeled for the late summer and early autumn months. A much less significant warming is calculated for the winter months. In the stratosphere, significant cooling is attributed to aviation CO_2 emissions which reaches −0.25 °C by the end of

ACPD
13, 3817–3858, 2013

the 21st century. A −0.3 °C temperature decrease is modeled when considering all the aviation emissions as well, but no significant signal is coming with CIC and NO_x emissions in the stratosphere.

1 Introduction

The environmental stress of global aviation has been a concern since the 60s, early 70s (Osmundsen, 1963; Johnston, 1971; Johnston and Quitevis, 1971). Since these pioneering studies, large progress has been achieved in the understanding of aviation impact on the environment that resulted in two major assessments. The first one was undertaken by the Intergovernmental Panel for Climate Change (IPCC, 1999) and, recently, Lee et al. (2010) provided a comprehensive report on the issue. They accounted for the impact of the emissions produced by aircraft on the atmospheric chemistry and climate only, however, aircraft produce significant noise, especially around airports, therefore the health effects of aircraft noise is subject to investigation in many studies as well (e.g. Roselund et al., 2001).

Emissions of gases and aerosols from global aviation altering the chemical composition of the atmosphere and, consequently, the change of abundances in the radiatively active gases and aerosols, have an impact on the radiative forcing (RF) and lead to temperature changes (Skeie et al., 2009). The condensation trail (contrail) formation from water vapor emissions and the induced cirrus cloud generate further RF from aviation.

The RF components from subsonic aviation originate from several processes (Lee et al., 2009). CO_2 (carbon dioxide) emissions increase the CO_2 levels and result in a positive RF. The range of 25.0–28.0 mW m^{-2} was provided by the studies of Sausen et al. (2005) and Lee et al. (2009) for the years 2000 and 2005. Emissions of NO_x (nitrogen oxides) trigger through a chain of chemical reactions the formation of O_3 (ozone) that produce a positive RF (Grewe et al., 2002a,b; Stevenson et al., 2004; Köhler et al., 2008; Myhre et al., 2011). Secondly, it causes a long-lived CH_4 (methane)

ACPD
13, 3817–3858, 2013

reduction that represents a negative RF (Stevenson et al., 2004). Finally, a long-term small O_3 decrease is attributed to this methane reduction resulting in a negative RF (Köhler et al., 2008). The RF estimates of the latter study for these three components are of 30 mW m^{-2}, −19 mW m^{-2} and −11 mW m^{-2}, respectively for the 2002 emissions. This gives a zero net forcing. Stevenson et al. (2004) reached the same conclusion indicating an overall low RF due to aviation NO_x emissions.

Aircraft emit water vapor (H_2O) that is a greenhouse gas with a positive RF estimated to 2.8 mW m^{-2} by Lee et al. (2009) for 2005. The most recent study, Wilcox et al. (2012) however updates H_2O vapor RF to a smaller value of 0.9 mW m^{-2}.

An important effect of aircraft H_2O emissions routinely observed is the formation of persistent contrails and contrail cirrus (Atlas et al., 2006). Contrails are line-shaped cirrus that form after the mixing of the hot and moist air from the aircraft engines with the ambient air while the Schmidt-Appelman criterion (Schumann, 1996) has to be fulfilled requiring the air being under a critical temperature. According to the local meteorological conditions, a contrail can undergo shear, uplift and mixing that results in its areal extent – a contrail cirrus is formed. The contrail ice nuclei can also modify the natural cirrus cloudiness (Boucher, 1999). Hereafter, we will use the term "Contrail Induced Cloudiness" (CIC) that will refer to contrails, contrail cirrus and natural cirrus modifications mentioned later. We have to point out that the term "Aviation Induced Cloudiness" (AIC) is defined as well (Lee et al., 2010) that adds aircraft soot generated cloudiness to CIC.

The detection (measurement), properties, formation, evolution and radiative effects of CIC have been subject to a large number of studies (Zerefos et al., 2003; Schumann, 2005; Stordal et al., 2005; Gao et al., 2006; Hong et al., 2008; Frömming et al., 2011). The physical mechanism behind its formation is now well understood but due to the uncertainties in the modeling of its occurrence and of its time/space varying properties, the calculation of the related RF is still marked with a low to very-low level of scientific understanding (Lee et al., 2010). Current RF estimates lie in the 10–80 mW m^{-2} interval

ACPD
13, 3817–3858, 2013

for the year 2005 (Lee et al., 2009). The most up-to-date CIC RF estimate is given by Burkhardt and Kärcher (2011), 31 mW m^{-2} for year 2005.

Aircraft black carbon (BC) emissions represent a tiny fraction of the total emitted anthropogenic BC mass, but BC particles originating from aircraft engines are much smaller than from other sources. Thus the number concentration of BC is perturbed significantly due to aviation (Hendricks et al., 2004). RF estimates for BC recently given by Balkanski et al. (2010), are of 0.1 or 0.3 mW m^{-2} depending on whether BC externally or internally mixed with sulphate is considered. In contrast, a one order larger negative RF is calculated by the same authors for aviation sulphate aerosols ($\sim$ 1 mW m^{-2}).

The total RF of aviation was evaluated by Sausen et al. (2005) for 2000, and recently by Lee et al. (2010) for 2005, giving positive RF of 47.8 mW m^{-2} and 55.0 mW m^{-2}, respectively. These values included linear contrails (around 10 mW m^{-2}) but excluded the aviation induced cirrus cloudiness that is very uncertain in terms of its related RF. The latter can be however estimated from the latest CIC estimate from Burkhardt and Kärcher (2011) to be of 21 mW m^{-2}. So the total RF from the aviation sector for the year 2005 is around 70–75 mW m^{-2}.

The above positive RF represents a considerable contribution to the total anthropogenic RF of 1660 mW m^{-2} (Lee et al., 2010) and it may be responsible for significant warming and other changes (e.g. precipitation). Furthermore, this forcing is expected to gradually increase towards the end of the 21th century (Skeie et al., 2009) therefore its impact might rise as well. The response of the climate system to a given radiative forcing is delayed due to its thermal inertia (Hansen et al., 2005). If the land-surface and the ocean mixed layer are only considered, the timescale of the response is of 1 to 5 yr (Olivié and Stuber, 2010). Taking into account the deep ocean response, this timescale changes to several centuries. In terms of intensity, the fast response contributes to 60–80 % of the total response. This inertial behavior has to be taken into account when modeling the transient phase of climate change (Olivié et al., 2012). A couple of studies considered this when investigating the climate impact of aviation emissions (Ponater et al., 2005, 2006; Lim et al., 2007; Skeie et al., 2009) but they used

ACPD
13, 3817–3858, 2013

simplified model approaches that cannot give answer about the geographic distribution of the impacts.

To investigate the long term response of a varying anthropogenic forcing (such as aviation), including its geographic and vertical distributions, a more sophisticated approach, the use of an AOGCM (Atmosphere-Ocean General Circulation Model) is required as it describes the atmosphere, ocean and sea-ice and the interactions between them in detail. This is certainly a computationally demanding task and for the aviation impact, Olivié et al. (2012) is one of the few studies that adopted this approach. They assessed the climate impact of all transport sectors (road, shipping and aviation) for the period 1860–2100. The AOGCM they applied did not contain detailed chemistry of the atmosphere but a simplified O_3 scheme (Cariolle and Teyssèdre, 2007). Therefore the forcing agents (like CO_2, aerosols etc.) perturbed by the specific transport sector were provided externally as global constants or 3-D fields. For ozone, two approaches were adopted: in the first one, they prescribed 3-D perturbed ozone fields, in the second one, the simplified ozone scheme was used. The CIC were not calculated online during the simulations, but an external data source served to track its presence in the model atmosphere and was later provided to the radiative code of the AOGCM.

Here we present a novel approach to evaluate the climate-chemistry impact of aviation emissions: we use a similar AOGCM to that of Olivié et al. (2012), the novelty being that, in our AOGCM, we consider online coupled chemistry limited to the mid-troposphere and stratosphere, regions that encompass the altitudes where the air-traffic and their emissions mostly occur. This allows us to use the aviation emissions as inputs to the model (i.e. not the concentration perturbations) and to account for all the chemical processes triggered by these emissions. Our main focus in this paper will be the 3-D temperature response to these aviation emissions, investigating the 1940–2100 period.

As forcing agents, we will consider CO_2, NO_x and CO emissions; they represent the vast majority of the material emitted from aircraft engines. We will account for water emissions only in the form of contrail ice particles and not as water vapor assuming its

ACPD
13, 3817–3858, 2013

radiative impact negligible as confirmed recently by Wilcox et al. (2012). Previous studies showed (see above) that aerosol originating from the aviation sector has a minor climate impact, so in our study aviation related aerosols (soot and sulphates) will not be considered. As in many transport related impact studies, we will distinguish between CO_2 and non-CO_2 impacts that represent the climate impact of the CO_2 emissions only and that of all other emissions. Further we present the NO_x impact, i.e. the impact of the NO_x emissions only, and the CIC impact, i.e. the impact of the contrails and the induced cirrus alone. Finally, the total aviation impact will be evaluated as well.

2 Tools and experimental set-up

2.1 Model CNRM-CM

In our work, we used the atmospheric-chemistry model coupled with an ocean/sea ice model, denoted as CNRM-CCM model hereafter. It is an extension of the Ocean/Atmosphere General Circulation Model CNRM-CM5.1 that is extensively described in Voldoire et al. (2012).

In summary, CNRM-CM is a state-of-the-art general circulation model that has been jointly developed by CNRM-GAME (Centre National de Recherches Météorologiques – Groupe d'études de l'Atmosphère Météorologique) and CERFACS (Centre Européen de Recherche et de Formation Avancée) in order to contribute to phase 5 of the Coupled Model Intercomparison Project (CMIP5, see http://cmip-pcmdi.llnl.gov/cmip5/experiment_design.html). CNRM-CM5.1 includes the atmospheric model ARPEGE-Climat (v5.2), the ocean model NEMO (v3.2; Madec, 2008), the land surface scheme ISBA and the sea ice model GELATO (v5; Salas, 2002) coupled through the OASIS (v3; Valcke, 2006) system. Horizontal resolution of the atmosphere is about 1.4° and 1° for the ocean. The atmospheric component uses the Morcrette et al. (2001) scheme over 6 bands for the solar radiation and the RRTM scheme for the long-wave radiation. Seven gases are considered as absorbers, H_2O, CO_2, O_3, CH_4, N_2O, CFC11, and CFC12.

ACPD
13, 3817–3858, 2013

O_3 is a prognostic variable with photochemical production and loss rates computed off-line by a 2-D zonal chemistry model (MOBIDIC; Cariolle and Teyssèdre, 2007). H_2O is a prognostic variable and the other 5 absorbents are prescribed to a uniform value that evolves on a yearly basis. The climatology of tropospheric aerosols from Szopa et al. (2012) is prescribed, while the land surface scheme has been externalised from the atmospheric model through the SURFEX platform. It includes new developments such as a parameterization of sub-grid hydrology, a new soil freezing scheme and the ECUME bulk parameterization for ocean surface fluxes.

2.2 CNRM-CM chemistry version: CNRM-CCM

The atmospheric model embedded in CNRM-CCM is the one used for CNRM-CM5, described in the previous paragraph. The main difference resides in the "online" coupling with a stratospheric chemistry which is based on the REPROBUS stratospheric chemistry scheme (Lefèvre et al., 1994). This chemistry is applied on the whole vertical column, except between the surface and the 700 hPa level where long-lived chemical species are relaxed towards global average surface value following the A1B scenario. Convection of species is not considered. In this chemistry version, the 3-D distribution of the seven absorbing gases is then provided by the chemistry module of CNRM-CCM and interacts with the radiative calculations. More details can be found in Michou et al. (2011).

In the CNRM-CM default version, there are only 31 vertical levels of which 5 are in the stratosphere. For stratospheric chemistry studies, the number of vertical levels has been increased to 60 layers (26 of them being in the stratosphere). This increase of vertical resolution requires to reduce the time-step from 30 to 15 min. Additionally, as there are about 50 3-D supplementary species, the horizontal resolution was reduced from 1.4°to 2.8°to reduce computational costs. As a consequence of the resolution decrease, the horizontal diffusion and gravity wave drag have been adjusted. To address the aviation impact, several aspects need to be added to the model: aircraft and lightning emissions and plume representation. These points are detailed in the following

ACPD
13, 3817–3858, 2013

paragraphs. Finally, this version of CNRM-CCM costs about 21 h of elapsed-time to simulate one year on the NEC supercomputers of Météo-France.

2.3 Emission data

The emission data we used were developed within the QUANTIFY project, an Integrated Project funded through the EU-Framework Programme 6 (Lee et al., 2005)(see http://www.ip-quantify.eu). For aviation, they consist in 3-D data with a horizontal resolution of $1^{\circ} \times 1^{\circ}$. and a 610 m vertical spacing up to 14 km.

These data contain monthly totals of fuel consumption and emissions for NO_x and soot as kg gridbox^{-1} month^{-1}. They are only available for years 2000, 2025, 2050, and 2100 (see Fig. 1 for the 2000 and 2100 horizontal and zonally averaged fuel consumption distribution). For the period 1940–2100, time series of global emission estimates are also included (see Fig. 2). In 1940, the emissions are identically zero, since this year is considered as the beginning of significant aviation activities (Sausen and Schumann, 2000). Until 2020, FESG forecast values are adopted (FESG, 2008), which assumes that the fuel efficiency continues with recent trends and that NO_x improvements commensurate with insertion of the best of present-day technology. The QUANTIFY dataset does not contain explicitly military aviation emissions, however the civil aviation emission patterns are scaled to the IEA aviation fuel-burn totals.

To provide 3-D emission data for other years than those available in the emission inventory (i.e. for the whole period 1940–2100), we linearly interpolated the emissions in time and normalized them with their annual totals.

When assessing the role of the NO_x aviation emissions, the lightning NO_x (LNO_x) has to be taken into account since several studies (Bernsten et al., 1999; Grewe, 2003; Schumann and Huntrieser, 2007) have shown that it is another major source of NO_x in the atmosphere. This has important implications for the atmospheric chemistry and climate and disregarding LNO_x while calculating the aviation NO_x impacts (which is about 5 times smaller than LNO_x for present days) could lead to erroneous conclusions (Grewe, 2003). Therefore, we consider LNO_x as well in our study. The data are

ACPD
13, 3817–3858, 2013

taken from the ANCAT lightning NO_x emission monthly climatology defined for the year 1992. For other years, we applied a scaling on the global mean surface temperature as suggested by Schumann and Huntrieser (2007) who estimate a 10% increase of lightning activity and emitted LNO_x by each 1 K of global mean surface temperature increase.

Emissions from aviation and lightning had to be implemented into CNRM-OACCM that originally did consider neither 2-D nor 3-D emissions. They are read in by the model at the beginning of each simulated month, interpolated to the model grid and converted to emissions densities that the model uses in the continuity equations to calculate the temporal evolution of the chemical species. We also adopted the temporal disaggregation of the monthly emission values given by Wilkerson et al. (2010). They provide weekly and hourly global profiles, so profiles are the same for every geographic region and reflect the evolution of the global emission value and not the actual local variation of the emissions.

2.4 Parameterizations

The small-scale processes during the dilution of the aircraft emission plume cannot be explicitly resolved in our experimental set-up due to our coarse model resolution. However, these processes can imply changes at the model resolved scale, e.g. can lead to modified chemical species concentrations and/or can consequently have radiative impacts.

One of these subgrid scale processes is the chemical evolution of the NO_x emissions in the aircraft engine plume and the subsequent ozone formation. It was shown by many authors (e.g. Kraabøl et al., 2002; Cariolle et al., 2009, and references therein) that disregarding the chemical non-linearities in the NO_x-plumes behind the aircraft by applying instantaneous dilution at the model scale (as it is usually done in chemistry transport models – CTM) leads to increased NO_x concentrations and ozone formation. Cariolle et al. (2009) developed a parameterization to account for this in large scale CTM. The method, that has been succesfully applied for the ship NO_x emissions as

ACPD
13, 3817–3858, 2013

well (Huszar et al., 2010), introduces a "fuel" tracer with a certain lifetime that traces the amount of material in the plume. The large scale NO_x and O_3 concentrations are then modified according to the concentration of this tracer using an effective reaction rate for the ozone formation. The method of Cariolle et al. (2009) has been implemented into CNRM-CCM.

Another aspect of the subgrid scale processes occurring in the aircraft plume is the condensation of water vapor emitted, and the subsequent formation of contrails and contrail cirrus (depending on the meteorological conditions). We have not considered a parameterization of the formation and evolution of the contrails, however as the radiative effects of the CIC are of great importance and cannot be neglected, we have developed a simplified treatment of these processes and their related radiative effects. Our method, similar to that of Olivié et al. (2012) is summarized below.

First we introduce a contrail tracer (in a similar way as the "fuel" tracer mentioned above) with a certain lifetime (15 h). The modeled distribution of this tracer on the 250 hPa level, representing the main flight level, is plotted in Fig. 3 (left). CIC is expected to form where temperature is less than −40 °C and the relative humidity exceeds 80 %. In model grid points fulfilling these conditions, we add the contrail tracer concentration, multiplied by a given factor, to the large scale cloud ice mixing ratio. The value of this multiplicative factor is tuned to obtain an appropriate annual global value of the top-of-the-atmosphere radiative forcing for the contrail and contrail induced cirrus for 2005. This target value is taken from Burkhardt and Kärcher (2011), 31 mW m^{-2}, representing the most recent estimate. This factor is held constant between 1940 and 2100. The distribution of the TOA radiative forcing due to CIC for the year 2005 is seen in Fig. 3.

As pointed out in the model description, the chemistry is resolved in the stratosphere down to the mid troposphere. Chemical processes are not considered in the lower troposphere where concentrations are relaxed towards climatological values which represent lower boundary conditions. When performing various simulations with perturbed aviation effects (e.g. simulations with/without aviation CO_2 emissions; see

ACPD
13, 3817–3858, 2013

further below), these lower boundary conditions have to reflect the situation that would occur if the whole troposphere was treated by explicit chemistry. In the case of CO_2, an increase occurs due to aircraft emissions, while in the case of methane, aircraft NO_x enhance OH concentrations which accelerate methane reduction through a chemical reaction with OH. Therefore we have prescribed the aviation CO_2 contribution and methane reduction in the tropospheric relaxation values.

For CO_2, Skeie et al. (2009), who uses the same emission inventory as in this study, provide the aviation CO_2 contribution until the end of the 21th century. The evolution of this contribution in ppmv is plotted in Fig. 4 (right, pink line).

The magnitude of the methane reduction due to aviation NO_x emissions has been calculated following Olivié et al. (2012). They used the hydroxyl radical perturbation due to aviation for present as well as for 2025 and 2050 conditions in 3 different CTMs (Hodnebrog et al., 2011) to calculate the methane lifetime reduction and its consequent reduction of concentration. For intermediate years from 1940 to 2100 we inter- and extrapolated the OH enhancement and therefore the methane changes.

We have to point out that these results did not consider the in-plume chemical non-linearities that we have mentioned earlier and which result in a lower OH enhancement and subsequently in a smaller methane reduction. Kraabøl et al. (2002) calculated that the change of the methane lifetime becomes ~ 9 % smaller when plume processes are considered. We used this correction in our methane lifetime reduction. The 1940–2100 evolution of the CO_2 and methane absolute concentrations as well as of the perturbations due to the aviation NO_x emissions with/without the NO_x-plume parameterization, for the A1B scenario, can be seen in Fig. 4 (right, blue line).

2.5 Model simulations

The goal of the study is to evaluate the aviation impact on chemistry and climate for the 1940–2100 period. This requires to perform several simulations with perturbed aviation emissions to quantify their effects. To do this, consistent initial conditions are essential

ACPD
13, 3817–3858, 2013

for the year 1940, both for the atmospheric part of the model including its chemical composition as well as for the ocean and the sea ice.

Another task before starting the "impact-simulations", i.e. the experiments over the period 1940–2100 considering the aviation emissions, is to ensure that the chosen model configuration is able to simulate the climate system reasonably without significant biases and trends when the forcings are set constant.

To meet these requirements, a 100-yr spinup was integrated under the 1860 conditions (i.e. greenhouse gas concentrations – GHG and solar constant). In this spinup, the online chemistry was turned off. After this spinup, the model was run further towards the end of the 21st century with forcings according to the A1B scenario. This experiment is denoted DEFnochem, as this simulation applied the default model that used standard GHG evolutions while no 3-D aviation emissions were explicitly supplied, which however means that the aviation impact was included implicitly through the prescribed GHG concentrations.

A simulation called DEFchem in which the chemistry scheme is activated has been started from year 1920 of DEFnochem. Years 1920–1940 are then considered as spinup years to allow the chemical composition of the atmosphere to be in equilibrium with the mean climate of the model. We have checked that 20 yr is enough to initialize the chemistry in order to have consistent initial conditions for 1940.

For the period 1940–2100 we performed several experiments with aviation forcings (CO_2, NO_x, CIC) turned off/on (i.e. whether the related emissions or the contrails are considered or not). These (as well as the default simulations) are summarized in Table 1.

All the effects are accounted for in the experiment denoted "ALL". In the noCIC experiment, the effect of contrails and contrail induced cirrus is removed. In the "noCICnoCO2" experiment we removed also the CO_2 emissions. The same was done with the NO_x emissions ("noCICnoNO$_x$"). At last, the "noAVIATION" experiment considers no aviation emissions at all.

ACPD
13, 3817–3858, 2013

In order to identify the climate signal caused by these effects, we have to account for the effect of the variability of the modeled climate. We achieved this by performing ensembles of 3 members for all "impact simulations" (1–5 in Table 1). A larger ensemble was impossible due to the computational costs of the experiments due to online coupled chemistry. These ensembles were performed over the 2000–2100 period, as we expect negligible impact of aviation for the 1940–1999 period following Olivié et al. (2012). The year 2000 perturbation required for the 2nd and the 3rd members of the mini-ensemble was obtained by restarting from 1 January 1999 and 2001 instead of 2000 as done in the 1st (original) member. Hereafter, results shown for the 2000–2100 period will by default represent ensemble means from these three simulations, unless explicitly stated otherwise.

The impact of an individual emission or all aviation emissions has been evaluated as a difference of appropriate experiments, in particular:

- CO_2-impact: noCIC experiment – noCICnoCO2 experiment
- NO_x-impact: noCIC experiment – noCICnoNOx experiment
- CIC impact: ALL experiment – noCIC experiment
- non-CO_2-impact: ALL experiment – noCICnoNOx experiment
- Total impact: ALL experiment – noAVIATION experiment

3 Results

3.1 Overall climate change since the preindustrial times

The modeled evolution of the global annual average near surface temperature (at 2 m) for the default experiments between 1860 and 2100 is plotted in Fig. 5. The modeled warming due to all anthropogenic forcing for both simulations, i.e. with/without online

ACPD
13, 3817–3858, 2013

chemistry with respect to 1860 is about 1.0, 2.5 and 4.5 °C for the years 2000, 2050 and 2100, respectively. This holds for the warming simulated by the DEFchem experiment as well, although by the end of the century this warming tends to be less than that of the experiment without online coupled chemistry (DEFnochem) by around 0.3–0.5 °C.

In the DEFnochem simulation, the Arctic sea-ice extent is generally over-estimated, especially over the Northern Atlantic. We attributed this bias to the large difference between the resolution of the atmospheric model (2.8° × 2.8°) and that of the sea ice model (1° × 1°). To prove this affirmation we performed a sensitivity run with 1.4° × 1.4° resolution for the atmospheric model and we found that this run does not exhibit this sea ice bias over the Arctics. As the atmospheric model calculates mean fluxes over grid boxes that may be only partially covered with sea-ice, this may not be appropriate for the grid cells of the sea ice model. This high sea-ice extent bias persisted in the model simulations throughout the 20th and 21st centuries.

3.2 The mean global impact of different aviation emissions

In this section we present the global mean temperature response due to different aviation emissions as the difference in the corresponding experiments (see previous section). Figure 6 shows these differences in the corresponding ensemble members (thin lines) and in the 11-yr running mean of the ensemble means (thick lines) for the temperature at the surface (2 m) and at selected pressure levels, i.e. 850, 500, 250, 100 and 10 hPa, between 2000 and 2100.

Aviation emissions represent a positive RF causing warming in the troposphere. In the 20th century this effect is considered rather negligible but, with increasing emissions and related RF, it is expected to reach significant levels towards the end of the 21th century (Skeie et al., 2009; Olivié et al., 2012). As seen in Fig. 6, in our simulations the modeled impact on the 11-yr running mean temperature exhibits large variability throughout the whole examined period. By performing three-member ensemble simulations for the 2000–2100 period we intended to augment the signal to noise ratio.

ACPD
13, 3817–3858, 2013

However, the variability in the temperature response is still very large, especially for the 2 m temperature.

In general, the increase of temperature due to aviation emissions is visible when considering the CIC effect, the non-CO_2 effect and all aviation related emissions (the "Total" impact). The temperature response is evident especially at higher levels of the troposphere, i.e. at 500 and 250 hPa. A warming of up to 0.1 °C is predicted for the last two decades of the 21st century due to CIC impact (blue line) or non-CO_2 impact (brown line).

The expected warming due to aviation CO_2 is visible only at the end of the 21st century, reaching about 0.1 °C at the surface and at higher levels in the troposphere. However, in the upper stratosphere (at 10 hPa), CO_2 emissions from aviation lead to significant cooling that reaches −0.25 °C.

Our modeling system does not simulate a significant change of global mean temperature due to aviation NO_x emissions. In the next section we show that this is probably connected to limiting the chemistry to the upper troposphere and the stratosphere and the fact that the tropospheric species, including methane, were prescribed. This imposed a large negative forcing due to methane reduction and, with the reduced ozone production, leaded to small radiative forcing due to aviation NO_x emissions and thus negligible temperature response. As a consequence, the non-CO_2 impact goes in line with the CIC impact reflecting that its major component – the NO_x emission impact – is small in our simulations.

Finally, the largest temperature response is simulated when considering all the aviation emissions (green line), up to a 0.2 °C warming at higher levels in the mid troposphere towards the end of the century, with a warming present during the entire period.

Above the main flight levels, aviation emissions cause a slight cooling at 100 hPa (−0.05 °C) and a much larger cooling at 10 hPa (−0.3 °C) near the end of the century. A slight cooling in the stratosphere is simulated for the CIC and non-CO_2 effects as well, reaching −0.05 to −0.1 °C at the end of the 21st century.

ACPD
13, 3817–3858, 2013

3.3 The three-dimensional structure of the aviation impact on the temperature of the atmosphere

The globally averaged impact of aviation does not provide a detailed picture of the spatial distribution of its magnitude and of the statistical significance of the changes. Here we choose three 20-yr periods: 1991–2010, 2031–2050 and 2080–2099 representing the present-day, near future and far future conditions. We examine the change of temperature averaged over these 20 yr due to aviation emissions. The analysis is performed for the near surface temperature and for the zonal means. In order to draw a picture of the seasonality of the impacts, we calculate the monthly variation of the temperature changes as well.

3.3.1 Spatial patterns of the near surface temperature changes

In Fig. 7, the change in the global near surface temperature due to different aviation emissions is presented for the three periods, corresponding to the three columns from left to right.

The figure shows that the CO_2-impact (first row) is very small in the present day decades with small areas of statistically significant changes. It becomes stronger in the near future resulting in a decrease in temperature. The strongest impact is simulated during the far future period: statistically significant warming occurs over large areas at low latitudes and the Antarctic (up to 0.2 °C), with an even higher warming around the South Pole, up to 0.4 °C. Cooling is limited to the Arctics.

The impact of aviation NO_x emissions (second row) on near surface temperature is small in general and statistically significant over small areas with both warmings and coolings, in the −0.3–0.3 °C range. The largest temperature changes (warmings) are modeled over the Arctic, especially in the near future.

The CIC impact of on the near surface temperature suggests warming, although it is statistically significant only over small regions. The warming can reach as much as 0.3–0.5 °C.

ACPD
13, 3817–3858, 2013

The non-CO_2 impact (Fig. 7, fourth row) resembles the CIC effect, reflecting the low NO_x-impact modeled in our study. This impact is however stronger than the CIC one, with warming often exceeding 0.6 °C over the Arctic. Over other regions, the non-CO_2 emissions are responsible for a warming around 0.1–0.2 °C in the far future, although the areas with significant changes are limited.

More significant impacts are obtained when considering the combined effects of the emissions (Fig. 7, bottom row). The warming near the surface is significant during each examined time-slice. It can be as high as 0.6 °C over some regions in each period, but the area of statistical significance increases towards the end of the century.

3.3.2 Zonal mean temperature changes due to aviation emissions

This section provides results on the zonally averaged temperature response over the three periods analyzed in the previous section. The results are presented in Fig. 8 where each row corresponds again to a particular emissions or their combinations (from top to bottom: CO_2, NO_x, CIC, non-CO_2 and Total impact). The figure suggests that aviation emissions are, in general, responsible for warming in the troposphere and cooling in the stratosphere. The main cause of the stratospheric cooling are the CO_2 emissions, and this is why this cooling is well expressed in the "Total" impact as well. It remains negligible in present day conditions, reaches −0.1 to −0.2 °C in the middle of the century, and becomes the strongest towards the end of the century (−0.3 to −0.4 °C). Taking into account all the aviation emissions, the stratospheric cooling is even more pronounced, reaching −0.6 °C in zonal average in the far future.

Statistically significant zonally averaged tropospheric warming is computed for the CO_2-impact only in 2080–2099, from 90° S to 40° N. This warming reaches 0.1 °C over the equatorial belt and becomes even stronger over the Antarctic.

The zonal temperature changes due to NO_x emissions are not significant, except for a warming over the Equator in the upper stratosphere (around 20–100 Pa).

The CIC caused zonal mean temperature changes encompass warmings in the present day conditions up to 0.1–0.2 °C over the equatorial latitudes. In 2031–2050

ACPD
13, 3817–3858, 2013

this warming becomes larger and significant at almost all latitudes, with higher values over the Northern Hemisphere (up to 0.3 °C). In the far future, the temperature increase due to CIC is well emphasized between 60° S and 60° N, encountering maxima (of 0.3–0.4 °C) over 40–50° N corresponding to the denser aviation routes (see Fig. 3).

The aviation non-CO_2 emission induced temperature changes are again very similar to the CIC impact in magnitude. Highest values of warming in the troposphere are modeled over the Northern Hemisphere with maxima over the Arctic in the near future, and around the main flight corridors in the far future where temperature increases up to 0.3–0.4 °C.

Apart from the well expressed decrease in the stratosphere, an intensive temperature increase due to all aviation emissions is encountered in the troposphere in each period. In near and far future it covers almost all latitudes, and it reaches maximal values over the Northern Hemisphere (0.4–0.6 °C) in the far future.

3.3.3 Seasonal dependence of the aviation impacts on temperature

Aviation emissions are not uniformly distributed along the year but show a monthly variation peaking in July-August and being lowest in January (Olsen et al., 2013) and this seasonal variation is represented in the emission data we use as well. Furthermore, the environmental conditions under which these emissions trigger further effects, like temperature, prevailing winds, humidity etc. vary by season as well. Therefore, we might also expect a seasonal dependence of the impacts of the aviation emissions as well. To evaluate this dependence, we plotted the change of the monthly variation of temperature (see Fig. 9) providing information about the seasonal variation of the impact at all altitudes.

The main features of the impacts seen in the previous paragraphs appear also in Fig. 9, i.e. (1) during 1991–2010 the low, statistically not significant impact for the CO_2 and NO_x emissions, and the stronger impacts for the CIC, the non-CO_2 and the total emissions; (2) in the far future, the stratospheric cooling due to CO_2 and Total emissions, and the largest tropospheric warming.

ACPD
13, 3817–3858, 2013

Figure 9 further shows that the CO_2 tropospheric impact is significant during late spring until autumn with a maximum around September. The CO_2 induced cooling in the stratosphere is significant in both the near and far future in all seasons.

For the NO_x impact, only a small area of significant warming in the stratosphere above 100 Pa is simulated, throughout most of the year.

The CIC impact is the largest during early autumn in the present day period and is increasing in the middle and far future, with a shift of the maximum values to June and July. A small but statistically significant temperature decrease during late spring and early summer appears in the stratosphere.

The seasonal dependence of the non-CO_2 impact is similar to the CIC impact with a maximum tropospheric warming in September, a second local maximum for the near future in June and a stronger warming in 2080–2099 peaking in the summer months. The stratospheric cooling is present as well.

The impact of all the emissions (total impact) is significant in every season, in both the troposphere and the stratosphere and practically in each examined period. The largest tropospheric warming occurs during October 1991–2010 and during the summer in the two future periods.

3.4 Impact on atmospheric chemistry

This section presents the changes in the amount and 3-dimensional distribution of relevant air pollutants due to aviation emissions. Focus is given to the CO_2 and NO_x emissions and the triggered ozone change.

Previous studies dealing with the aviation CO_2 impact considered it as uniformly distributed over the globe (e.g. Olivié et al., 2012) given its long lifetime. However, to some extent the aviation contribution to the CO_2 distribution is not uniform and its maximum is concentrated in the Northern Hemisphere. Figure 10 presents the zonally averaged aviation CO_2 contribution in ppmv for 1991–2010, 2031–2050 and 2080–2099. The highest impact is located at the main flight levels over the Northern Hemisphere, where the maximum CO_2 contribution is around 1.5, 5.5 and 20 ppmv, respectively in the three

ACPD
13, 3817–3858, 2013

periods. In the troposphere, the contribution goes down to 1.4, 5.3 and 19.5 ppmv, while in the stratosphere it decreases to 1.1, 4.6 and 17.8 ppmv, respectively.

The zonally averaged impact of aircraft NO_x emissions on the NO_x and ozone concentrations is presented in Fig. 11. For NO_x, significant changes occur at the main flight levels over the Northern Hemisphere, becoming important in the Southern Hemisphere as well in 2080–2099. The contribution reaches 50, 100 and 150 pptv for the three periods, respectively. Regions of significant changes occur in the stratosphere as well, with a decrease up to −30 pptv in the near future and an increase over 100 pptv in the far future.

The aviation induced, zonally averaged ozone changes (Fig. 11, bottom row) are very small in the 1991–2010 period reaching 0.5 ppbv and being significant only at the main flight corridors in the Northern Hemisphere. A more pronounced contribution is modeled for 2031–2050 with statistically significant contributions over 20 ppbv. In 2080–2099 the aviation ozone contribution reaches only 10 ppbv over the Northern Hemisphere, but a strong ozone increase is modeled in the stratosphere above 100 Pa reaching a similar value around 10 ppbv.

4 Discussion and conclusions

The presented work assesses the impact of the global aviation on climate, focusing on the atmospheric temperature changes, and using an AOGCM with online coupled chemistry. Previous studies used either simplified climate models or uniformly distributed GHGs in AOGCMs to examine this impact.

The total anthropogenic impact expressed in terms of changes in near surface temperatures corresponds well with IPCC (2007) values. Olivié et al. (2012) with an earlier version of our AOGCM simulated slightly higher global mean near surface temperature values (around 13.5–14 °C in 1860) as we have a larger sea ice extent in our experiments. However, by the end of the 21st century, estimations become similar indicating a stronger warming in our experiments.

ACPD
13, 3817–3858, 2013

The globally averaged impact of aviation on temperatures shows high variability and the signal is clearer over higher altitudes. We did not obtain such a unique warming for aviation CO_2 and non-CO_2 effects as in Olivié et al. (2012), however our impact is usually of the same magnitude as in their study. With online chemistry our model has more degrees of freedom thus the climate response to a "small" forcing may be less pronounced because of the increased variability of the system.

For the CO_2 effects, a significant warming near the surface is modeled only in the 2080–2099 period, while a cooling appears in the middle of the century, especially over the Arctic. This confirms a result of Olivié et al. (2012) and may be connected to some complex feedback mechanism. The warming is pronounced especially over the Antarctics and the tropics at altitudes corresponding to the main flight levels, reaching 0.1 °C in zonal mean. The cooling in the stratosphere can be attributed to trapping the longwave radiation by the additional CO_2. Another finding is that the tropospheric warming is most significant during late Northern Hemisphere summer, probably because here, most of the emissions occur and often clear sky conditions govern during this time making the radiative effects of CO_2 stronger.

The impact of aviation NO_x emissions is very small, smaller than in previous studies. This holds also for the consequent O_3 changes. We imposed tropospheric methane relaxation values using the information from other global chemistry transport models that calculate the whole tropospheric chemistry, in contrary with our case where the chemical calculations are limited to mid-troposphere and stratosphere only. This prescribed methane changes are probably too large countering the aviation NO_x induced ozone formation. Consequently the radiative effects of too high methane reduction and small ozone production lead to non-significant NO_x impact on temperature.

The impact of contrails and contrail induced cloudiness (CIC) is clear in our simulations with a well pronounced warming in the whole troposphere up to 0.3 °C in zonal mean at the end of the 21st century. The warming near the surface is however not statistically significant everywhere. The highest impacts are modeled for the Northern Hemisphere around the flight corridors. In contrast with the aviation CO_2

ACPD
13, 3817–3858, 2013

induced stratospheric cooling, no CIC stratospheric cooling was detected. This can be explained by the different mechanism that lead to the CIC's radiative effect. The highest impact of CIC is simulated for the northern hemispheric summer, again probably because of more frequent clear sky conditions and peaking aviation transport.

The non-CO_2 impact is very similar to the CIC impact in our simulations, reflecting the low NO_x impact, as the non-CO_2 effects are made by CIC and NO_x emissions in our experiments and we do not consider aviation aerosol emissions.

The total impact of aviation emissions are represented by a well pronounced warming in the troposphere which is statistically significant in both present and future decades. Near the surface, the warming reaches around 0.2 °C by the end of the century, which is a lower value than given by the corresponding scenario in Skeie et al. (2009) (0.3 °C) who used a simple climate model for their calculations. The stratospheric cooling is also well expressed and resembles the cooling seen in case of the CO_2 impact. This cooling reaches −0.3 °C by the end of the century.

Our experiments indicate that the temperature response due to a radiative forcing may have in general a different geographical pattern than that of the radiative forcing itself. This is especially the case for the CO_2 impact where the maximum aviation CO_2 contribution is seen over the Northern Hemisphere but the larger warming is modeled over the southern one. Boer and Yu (2003) arrived to similar conclusions finding the structure of the temperature response to long lived green-house gases different from the structure of the forcing.

The aviation NO_x impact was probably underestimated in our experiments due to incomplete chemistry which excluded the lower tropospheric chemical reactions. To improve this study, a full tropospheric-stratospheric chemistry has to be considered when assessing the aviation climate-chemistry impact.

Another shortcoming to solve in future work is the difference in the horizontal resolutions of the atmospheric and ocean models that provided improper atmosphere-ocean fluxes causing a large sea ice bias in our experiments. A wrong reference state of sea ice may strongly bias the near surface temperature impact of aviation.

ACPD
13, 3817–3858, 2013

Finally, a more accurate treatment of contrail and contrail induced cloudiness is necessary for future assessments of the aviation impact.

Acknowledgements. This work has been performed within the "Impact du Transport Aérien sur l'Atmos-phère et le Climat" (ITAAC) project with support from the "Réseau Thématique de Recherche Avancée Science et Technologie pour l'Aéronautique et l'Espace" fundation. We further acknowledge the funding from the Ministry of Education of the Czech Republic (Research Plan No. MSM 0021620860) as well as the program PRVOUK – Environmental Reasearch of the Charles University in Prague. Authors wish to thank for the work of Activity 1 in the QUANTIFY project for creating aviation emission estimates.

The publication of this article is financed by CNRS-INSU.

References

Atlas, D., Wang, Z., and Duda, D. P.: Contrails to cirrus morphology, microphysics, and radiative properties, J. Appl. Meteor. Climatol., 45, 5–19, 2006. 3820

Balkanski, Y., Myhre, G., Gauss, M., Rädel, G., Highwood, E. J., and Shine, K. P.: Direct radiative effect of aerosols emitted by transport: from road, shipping and aviation, Atmos. Chem. Phys., 10, 4477–4489, doi:10.5194/acp-10-4477-2010, 2010. 3821

Berntsen, T. K. and Isaksen, I. S. A.: Effects of lightning and convection on changes in upper tropospheric ozone due to aircraft, Tellus B, 51, 766–788, 1999. 3825

Boer, G. J. and Yu, B.: Climate sensitivity and response, Clim. Dynam., 20, 415–429, doi:10.1007/s00382-002-0283-3, 2003. 3839

Boucher, O.: Air traffic may increase cirrus cloudiness, Nature, 397, 30–31, 1999. 3820

ACPD
13, 3817–3858, 2013

Burkhardt, U. and Kärcher, B.: Global radiative forcing from contrail cirrus, Nature Clim. Change, 1, 54–58, doi:10.1038/NCLIMATE1086, 2011. 3821, 3827

Cariolle, D. and Teyssèdre, H.: A revised linear ozone photochemistry parameterization for use in transport and general circulation models: multi-annual simulations, Atmos. Chem. Phys., 7, 2183–2196, doi:10.5194/acp-7-2183-2007, 2007. 3822, 3824

Cariolle, D., Caro, D. Paoli, R., Hauglustaine, D. A., Cuénot, B., Cozic, A., and Paugam, R.: Parameterization of plume chemistry into large-scale atmospheric models: application to aircraft NO_x emissions, J. Geophys. Res., 114, D19302, doi:10.1029/2009JD011873, 2009. 3826, 3827

FESG: ICAO/CAEP Forecasting and Economic Sub-Group (FESG) CAEP/8 Traffic and fleet forecasts Paper presented to CAEP Steering Group 19/08/08. ref. CAEP-SG/20082-IP/02, 2008. 3825

Frömming, C., Ponater, M., Burkhardt, U., Stenke, A., Pechtl, S., and Sausen, R.: Sensitivity of contrail coverage and contrail radiative forcing to selected key parameters, Atmos. Environ., 45, 1483–1490, 2011. 3820

Gao, R. S., Fahey, D. W., Popp, P. J., Marcy, T. P., Herman, R. L., Weinstock, E. M., Smith, J. B., Sayres, D. S., Pittman, J. V., Rosenlof, K. H., Thompson, T. L., Bui, P. T., Baumgardner, D. G., Anderson, B. E., Kok, G., and Weinheiner, A. J.: Measurements of relative humidity in a persistent contrail, Atmos. Env., 40, 1590–1600, 2006. 3820

Grewe, V.: Lightning NO_x emissions and the impact on the effect of aircraft emissions – Results from the EU-Project TRADEOFF. Proceedings of the AAC-Conference, 30 June to 3 July, Friedrichshafen, Germany, 2003. 3825

Grewe, V., Dameris, M., Fichter, C., and Sausen, R.: Impact of aircraft NO_x emissions. Part 1: interactively coupled climate-chemistry simulations and sensitivities to climate-chemistry feedback, lightning and model resolution, Meteorol. Z., 11, 177–186, 2002a. 3819

Grewe, V., Dameris, M., Fichter, C., and Lee, D. S.: Impact of aircraft NO_x emissions. Part 2: effects of lowering the flight altitude, Meteorol. Z., 11, 197–205, 2002b. 3819

Grewe, V., Shindell, D. T., and Eyring, V.: The impact of horizontal transport on the chemical composition in the tropopause region: lightning NO_x and streamers, Adv. Space Res., 33, 1058–1061, 2004.

Hansen, J., Nazarenko, L., Ruedy, R., Sato, M., Willis, J., Del Genio, A., Koch, D., Lacis, A., Lo, K., Menon, S., Novakov, T., Perlwitz, J., Russell, G., Schmidt, G. A., and Tausnev, N.:

ACPD
13, 3817–3858, 2013

Earth's Energy Imbalance: Confirmation and Implications, Science, 308, 1431–1435, doi:10.1126/science.1110252, 2005. 3821

Hendricks, J., Kärcher, B., Döpelheuer, A., Feichter, J., Lohmann, U., and Baumgardner, D.: Simulating the global atmospheric black carbon cycle: a revisit to the contribution of aircraft emissions, Atmos. Chem. Phys., 4, 2521–2541, doi:10.5194/acp-4-2521-2004, 2004. 3821

Hodnebrog, Ø., Berntsen, T. K., Dessens, O., Gauss, M., Grewe, V., Isaksen, I. S. A., Koffi, B., Myhre, G., Olivié, D., Prather, M. J., Pyle, J. A., Stordal, F., Szopa, S., Tang, Q., van Velthoven, P., Williams, J. E., and Ødemark, K.: Future impact of non-land based traffic emissions on atmospheric ozone and OH – an optimistic scenario and a possible mitigation strategy, Atmos. Chem. Phys., 11, 11293–11317, doi:10.5194/acp-11-11293-2011, 2011. 3828

Hong, G., Yang, P., Minnis, P., Hu, Y. X., and North, G.: Do contrails significantly reduce daily temperature range?, Geophys. Res. Letter., 35, L23815, doi:10.1029/2008GL036108, 2008. 3820

Huszar, P., Cariolle, D., Paoli, R., Halenka, T., Belda, M., Schlager, H., Miksovsky, J., and Pisoft, P.: Modeling the regional impact of ship emissions on NO_x and ozone levels over the Eastern Atlantic and Western Europe using ship plume parameterization, Atmos. Chem. Phys., 10, 6645–6660, doi:10.5194/acp-10-6645-2010, 2010. 3827

IPCC: Aviation and the global atmosphere, in: Intergovernmental Panel on Climate Change, edited by: Penner, E., Lister, J., Griggs, D. H., Griggs, D. J., Dokken, D. J., and McFarland, M., Cambridge University Press, Cambridge, UK, 1999. 3819

IPCC: Climate change 2007: the physical science basis. Contribution of working group I to the fourth assessment report of the intergovernmental panel on climate change, Cambridge University Press, Cambridge, UK and New York, NY, USA, 2007. 3837

Johnston, H.: Reduction of stratospheric ozone by nitrogen oxide catalysts from supersonic transport exhaust, Science, 173, 3996, doi:10.1126/science.173.3996.517, 1971. 3819

Johnston, H. S. and Quitevis, E.: The Oxides of Nitrogen with Respect to Urban Smog, Supersonic Transports, and Global Methane. International Congress of Radiation Research, US Department of Transportation and US Atomic Energy Committee, Seattle, Washington, 14–20 July 1974. 3819

Jones, P. W.: Conservative remapping: first-and second-order conservative remapping, Mon. Weather. Rev., 127, 2204–2210, 1999.

ACPD
13, 3817–3858, 2013

Köhler, M. O., Rädel, G., Dessens, O., Shine, K. P., Rogers, H. L., Wild, O., and Pyle, J. A.: Impact of perturbations to nitrogen oxide emissions from global aviation, J. Geophys. Res., 113, D11305, doi:10.1029/2007JD009140, 2008. 3819, 3820

Kraabøl, A. G., Berntsen, T. K., Sundet, J. K., and Stordal, F.: Impacts of NO_x emissions from subsonic aircraft in a global three-dimensional chemistry transport model including plume processes, J. Geophys. Res., 107, 4655, doi:10.1029/2001JD001019, 2002. 3826, 3828

Lee, D. S., Owen, B., Graham, A., Fichter, C., Lim, L. L., and Dimitriu, D.: Allocation of International Aviation Emissions from Scheduled Air Traffic – Present Day and Historical (Report 2 of 3), Manchester Metropolitan University, Centre for Air Transport and the Environment, Manchester, UK, 2005. 3825, 3848

Lee, D. S., Fahey, D. W., Forster, P. M., Newtone, P. J., Wit, R. C. N., Lim, L. L., Owen, B., and Sausen, R.: Aviation and global climate change in the 21st century, Atmos. Environ. 43, 3520–3537, 2009. 3819, 3820, 3821

Lee, D. S., Pitari, G., Grewe, V., Gierens, K., Penner, J. E., Petzold, A., Prather, M. J., Schumann, U., Bai, A., Berntsen, T., Iachetti, D., Lim, L. L., and Sausen, R.: Transport impacts on atmosphere and climate: aviation, Atmos. Environ., 44, 4678–4734, 2010. 3819, 3820, 3821

Lefèvre, F., Brasseur, G. P., Folkins, I., Smith, A. K., and Simon, P.: Chemistry of the 1991–1992 stratospheric winter: three-dimensional model simulations, J. Geophys. Res., 99, 8183–8195, 1994. 3824

Lim, L., Lee, D. S., Sausen, R., and Ponater, M.: Quantifying the effects of aviation on radiative forcing and temperature with a climate response model, in: Proceedings of an international conference on transport, atmosphere and climate (TAC), edited by: Sausen, R., Blum, A., Lee, D. S., and Brüning, C., 202–207, http://www.pa.op.dlr.de/tac/proceedings.html, 2007. 3821

Madec, G.: NEMO ocean engine. Note du Pole de modelisation, Institut Pierre-Simon Laplace (IPSL), France, No 27 ISSN No 1288–1619, 2008. 3823

Michou, M., Saint-Martin, D., Teyssèdre, H., Alias, A., Karcher, F., Olivié, D., Voldoire, A., Josse, B., Peuch, V.-H., Clark, H., Lee, J. N., and Chéroux, F.: A new version of the CNRM Chemistry-Climate Model, CNRM-CCM: description and improvements from the CCMVal-2 simulations, Geosci. Model Dev., 4, 873–900, doi:10.5194/gmd-4-873-2011, 2011. 3824

Morcrette, J.-J., Mlawer, E. J., Iacono, M. J., and Clough, S. A.: Impact of the radiation-transfer scheme RRTM in the ECMWF forecasting system, ECMWF Newsletter No. 91, Summer 2001. 3823

ACPD
13, 3817–3858, 2013

Myhre, G., Shine, K. P., Rädel, G., Gauss, M., Isaksen, I. S. A., Tang, Q., Prather, M. J., Williams, J. E., van Velthoven, P., Dessens, O., Koffi, B., Szopa, S., Hoor, P., Grewe, V., Borken-Kleefeld, J., Berntsen, T. K., and Fuglestvedt, J. S.: Radiative forcing due to changes in ozone and methane caused by the transport sector, Atmos. Environ., 45, 387–394, doi:10.1016/j.atmosenv.2010.10.001, 2011. 3819

Olivié, D. and Stuber, N.: Emulating AOGCM results using simple climate models, Clim. Dynam., 35, 1257–1287, doi:10.1007/s00382-009-0725-2, 2010. 3821

Olivié, D. J. L., Cariolle, D., Teyssèdre, H., Salas, D., Voldoire, A., Clark, H., Saint-Martin, D., Michou, M., Karcher, F., Balkanski, Y., Gauss, M., Dessens, O., Koffi, B., and Sausen, R.: Modeling the climate impact of road transport, maritime shipping and aviation over the period 1860–2100 with an AOGCM, Atmos. Chem. Phys., 12, 1449–1480, doi:10.5194/acp-12-1449-2012, 2012. 3821, 3822, 3827, 3828, 3830, 3831, 3836, 3837, 3838

Olsen, S. C., Wuebbles, D. J., and Owen, B.: Comparison of global 3-D aviation emissions datasets, Atmos. Chem. Phys., 13, 429–441, doi:10.5194/acp-13-429-2013, 2013. 3835

Osmundsen, J. A.: Weather Scientists are Optimistic that New Findings are Near, New York Times, 23 September, p. 1, 1963. 3819

Owen, B., Lee, D. S., and Lim, L.: Flying into the future: aviation emissions scenarios to 2050, Environ. Sci. Technol., 44, 2255–2260, doi:10.1126/science.1196285, 2010. 3849

Ponater, M., Marquart, S., Sausen, R., and Schumann, U.: On contrail climate sensitivity, Geophys. Res. Lett., 32, L10706, doi:10.1029/2005GL022580, 2005. 3821

Ponater, M., Pechtl, S., Sausen, R., Schumann, U., and Hüttig, G.: A state-of-the-art assessment of the potential of the cryoplane technology to reduce aircraft climate impact, Atmos. Environ., 40, 6928–6944, 2006. 3821

Rosenlund, M., Berglind, N., Pershagen, G., Järup, L., and Bluhm, G.: Increased prevalence of hypertension in a population exposed to aircraft noise, Occup. Environ. Med., 58, 769–773, doi:10.1136/oem.58.12.769, 2001. 3819

Salas, D.: A global coupled sea ice-ocean model, Ocean Model, 4, 137–172, 2002. 3823

Sausen, R. and Schumann, U.: Estimates of the climate response to aircraft CO_2 and NO_x emissions scenarios, Clim. Change, 44, 27–58, 2000. 3825

Sausen, R., Isaksen, I., Grewe, V., Hauglustaine, D., Lee, D. S., Myhre, G., Köhler, M. O., Pitari, G., Schumann, U., Stordal, F., and Zerefos, C.: Aviation radiative forcing in 2000: an update of IPCC (1999), Meteorol. Z., 14, 555–561, 2005. 3819, 3821

ACPD
13, 3817–3858, 2013

Schumann, U.: On conditions for contrail formation from aircraft exhausts, Meteorol. Z., 5, 4–23, 1996. 3820
Schumann, U.: Formation, properties and climatic effects of contrails, C. R. Physique 6, 549–565, 2005. 3820
Schumann, U. and Huntrieser, H.: The global lightning-induced nitrogen oxides source, Atmos. Chem. Phys., 7, 3823–3907, doi:10.5194/acp-7-3823-2007, 2007. 3825, 3826
Skeie, R. B., Fuglestvedt, J., Berntsen, T., Lund, M. T., Myhre, G., and Rypdal, K.: Global temperature change from the transport sectors: Historical development and future scenarios, Atmos. Environ., 43, 6260–6270, 2009. 3819, 3821, 3828, 3831, 3839
Stevenson, D. S., Doherty, R. M., Sanderson, M. G., Collins, W. J., Johnson, C. E., and Derwent, R. G.: Radiative forcing from aircraft NO_x emissions: mechanisms and seasonal dependence, J. Geophys. Res. 109, D17307, doi:10.1029/2004JD004759, 2004. 3819, 3820
Stordal, F., Myhre, G., Stordal, E. J. G., Rossow, W. B., Lee, D. S., Arlander, D. W., and Svendby, T.: Is there a trend in cirrus cloud cover due to aircraft traffic?, Atmos. Chem. Phys., 5, 2155–2162, doi:10.5194/acp-5-2155-2005, 2005. 3820
Szopa, S., Cozic, A., Shulz, M., Balkanski, Y., and Hauglustaine, D.: Aerosol and ozone changes as forcing for climate evolution between 1850 and 2100, Clim. Dynam., doi:10.1007/s00382-012-1408-y, in press, 2012. 3824
SPARC: SPARC CCMVal Report on the Evaluation of Chemistry-Climate Models: edited by: Eyring, V., Shepherd, T. G., and Waugh, D. W., SPARC Report No. 5, WCRP-132, WMO/TD-No. 1526, available at: http://www.atmosp.physics.utoronto.ca/SPARC, 2010.
Valcke, S.: OASIS3 user guide (prism_2-5). Technical report TR/CMGC/06/73, CERFACS, Toulouse, France, 60, 2006. 3823
Voldoire, A., Sanchez-Gomez, E., Salas y Mélia, D., Decharme, B., Cassou, C., Sénési, S., Valcke, S., Beau, I., Alias, A., Chevallier, M., Déqué, M., Deshayes, J., Douville, H., Fernandez, E., Madec, G., Maisonnave, E., Moine, M.-P., Planton, S., Saint-Martin, D., Szopa, S., Tyteca, S., Alkama, R., Belamari, S., Braun, A., Coquart, L., and Chauvin, F.: The CNRM-CM5.1 global climate model: description and basic evaluation, Clim. Dynam., doi:10.1007/s00382-011-1259-y, 2012. 3823
Wilcox, L. J., Shine, K. P., and Hoskins, B. J.: Radiative forcing due to aviation water vapour emissions, Atm. Env., 63, 1–13, doi:10.1016/j.atmosenv.2012.08.072, 2012. 3820, 3823
Wilkerson, J. T., Jacobson, M. Z., Malwitz, A., Balasubramanian, S., Wayson, R., Fleming, G., Naiman, A. D., and Lele, S. K.: Analysis of emission data from global commercial aviation:

ACPD
13, 3817–3858, 2013

2004 and 2006, Atmos. Chem. Phys., 10, 6391–6408, doi:10.5194/acp-10-6391-2010, 2010. 3826

Zerefos, C. S., Eleftheratos, K., Balis, D. S., Zanis, P., Tselioudis, G., and Meleti, C.: Evidence of impact of aviation on cirrus cloud formation, Atmos. Chem. Phys., 3, 1633–1644, doi:10.5194/acp-3-1633-2003, 2003. 3820

ACPD
13, 3817–3858, 2013

Table 1. Simulations performed in the study, simulated years, presence of online chemistry and of aviation forcings.

No.	Simulation ID	Period	Chemistry	CIC	CO_2	NO_x
1	ALL	1940–2099	yes	yes	yes	yes
2	noCIC	1940–2099	yes	no	yes	yes
3	noCICnoCO2	1940–2099	yes	no	no	yes
4	noCICnoNOx	1940–2099	yes	no	yes	no
5	noAVIATION	1940–2099	yes	no	no	no
6	DEFnochem	1860–2099	no	no	–	–
7	DEFchem	1920–2099	yes	no	–	–

ACPD
13, 3817–3858, 2013

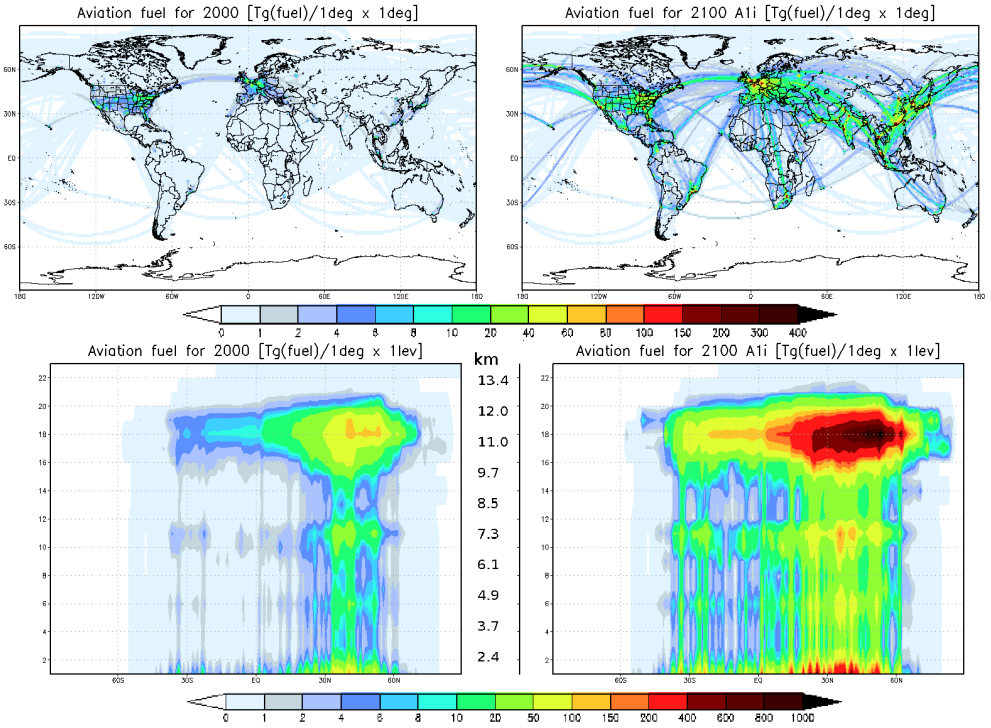

Fig. 1. Vertically (upper row) and zonally (bottom row) integrated aviation fuel consumption (Tg (fuel) yr^{-1}) for the years 2000 (left) and 2100 (right) assuming the A1(i) scenario (Lee et al., 2005).

ACPD
13, 3817–3858, 2013

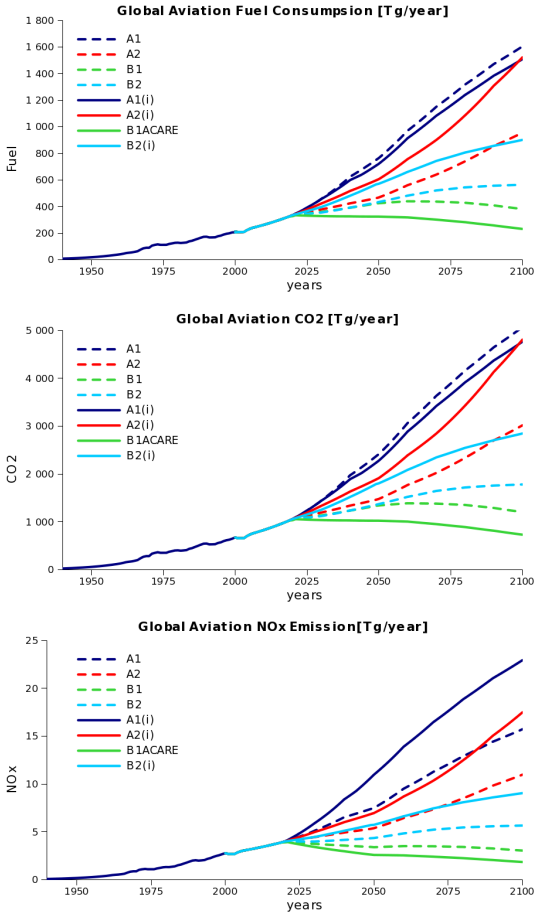

Fig. 2. Global annual fuel consumption, CO_2 and NO_x emissions ($Tg\,yr^{-1}$) from aviation for the period 1940–2100 for different scenarios (Owen et al., 2010).

ACPD
13, 3817–3858, 2013

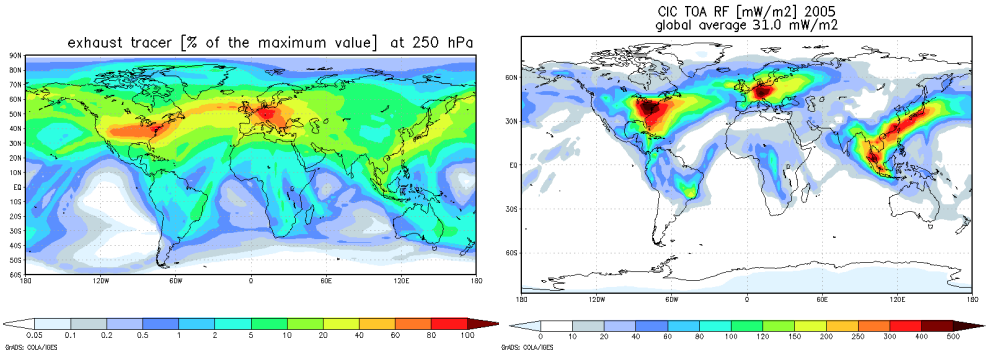

Fig. 3. On the left, annual mean horizontal distribution of the contrail tracer at 250 hPa as percentage of the maximum value. On the right, annual average TOA radiative forcing of CIC in mW m^{-2}. Both figures are for the year 2005.

ACPD
13, 3817–3858, 2013

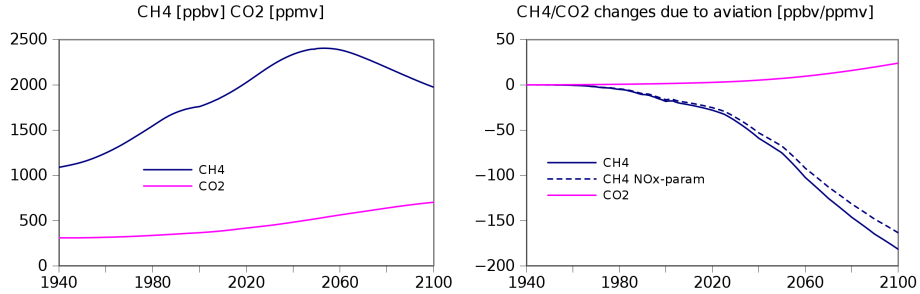

Fig. 4. On the left: evolution of methane and CO_2 according to the A1B scenarios. On the right: calculated methane reduction due to aviation NO_x emissions for the A1B scenario with (dashed line) and without (bold lines) NO_x plume parameterization; and CO_2 changes according to the A1(i) scenario.

ACPD
13, 3817–3858, 2013

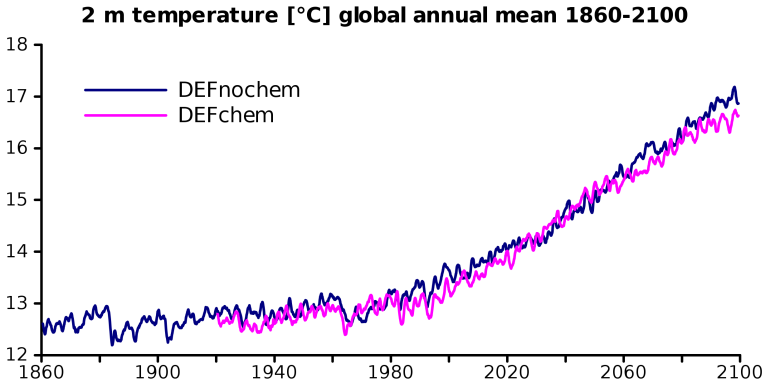

Fig. 5. Near surface (at 2 m) temperature evolution between 1860 and 2100 calculated by CNRM-CCM from the default simulations (DEFnochem and DEFchem).

ACPD
13, 3817–3858, 2013

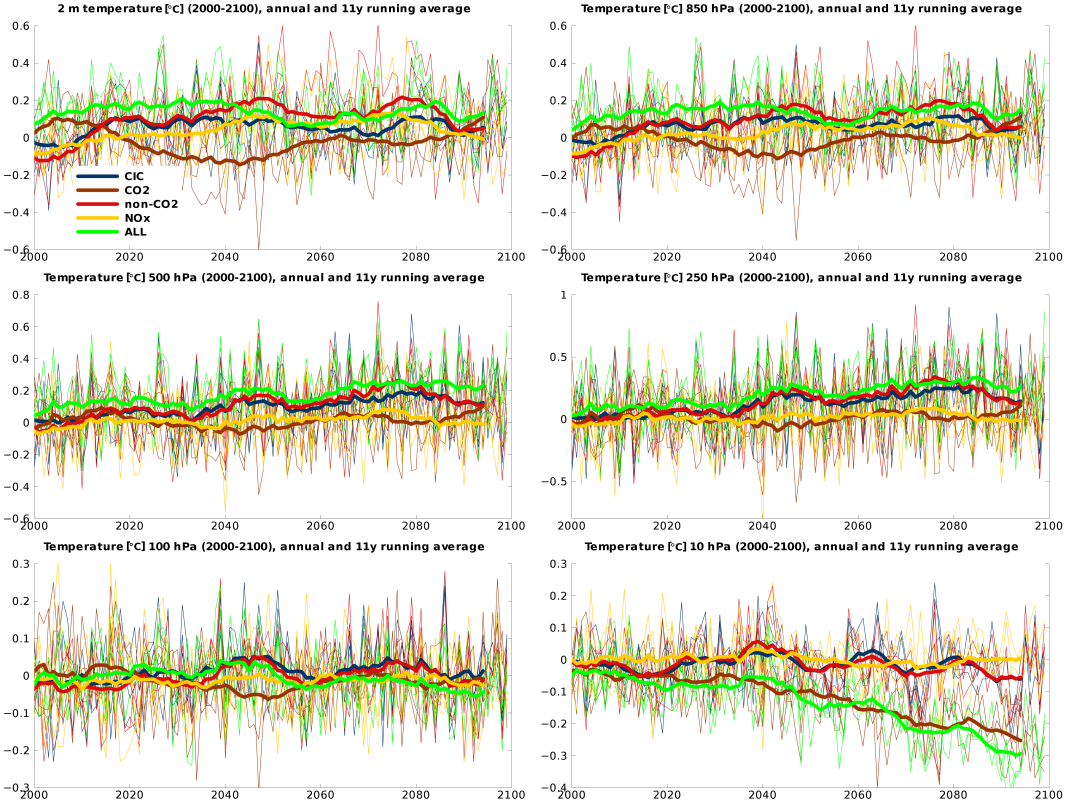

Fig. 6. Time series of the aviation emissions impact on global temperature between 2000 and 2100 at six different pressure levels. Thin lines indicate the annual impact from each of the three members of a simulation, and the thick lines indicate the 11-yr running average of the ensemble mean.

ACPD
13, 3817–3858, 2013

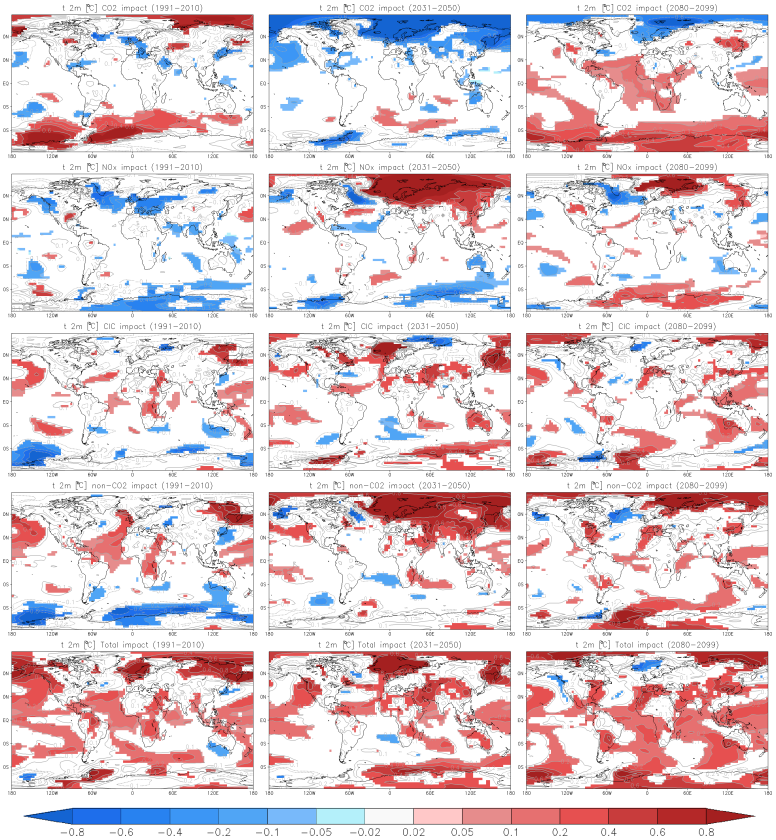

Fig. 7. Impact of aviation on near surface temperature averaged over 1991–2010 (left column), 2031–2050 (middle column) and 2088–2099 (right column). Rows represent the CO_2 (first row), NO_x (second row), CIC (third row), non-CO_2 (fourth row) and all the aviation effects (fifth row). The shaded areas correspond to statistically significant changes at the 90 % level of confidence applying a t-test.

ACPD
13, 3817–3858, 2013

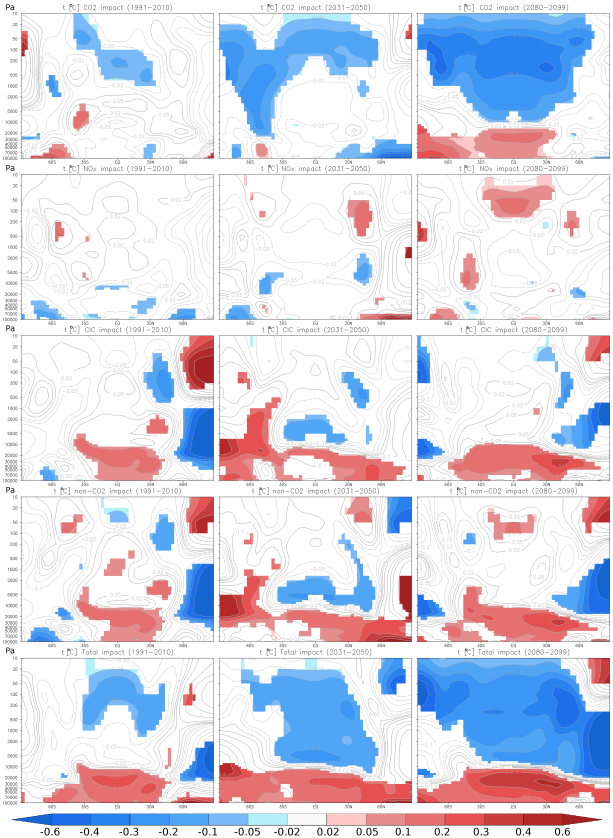

Fig. 8. Zonally averaged impact of aviation emissions on temperature over 1991–2010 (left column), 2031–2050 (middle column) and 2088–2099 (right column). The rows (from top to bottom) represent the impact of CO_2, of NO_x emission, of CIC, of the non-CO_2 emissions and of the all the emissions considered (total impact). The vertical axis corresponds to pressure in Pa. The shaded areas represent statistically significant changes at the 90 % level of confidence applying t-test.

ACPD
13, 3817–3858, 2013

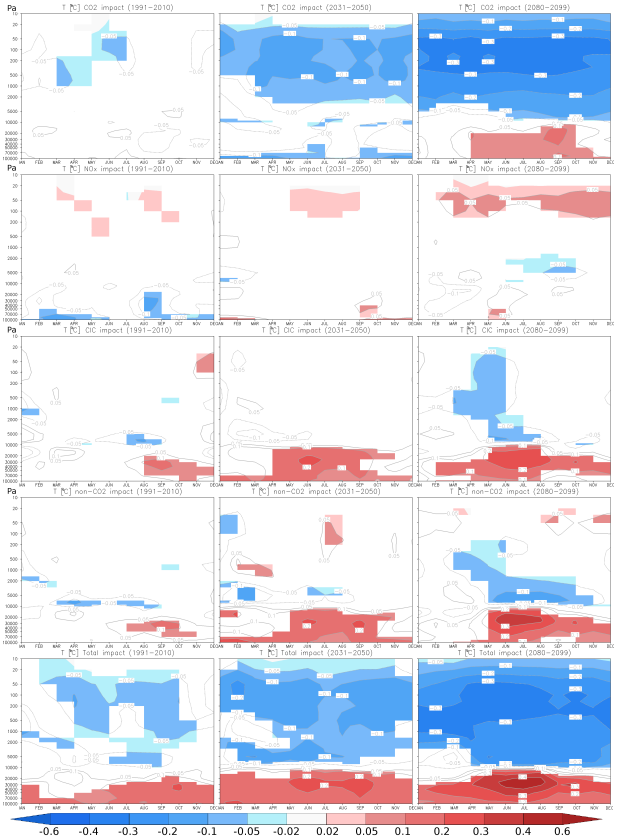

Fig. 9. Impact on the monthly global vertical profile of temperature due to aviation emissions averaged over 1991–2010 (left column), 2031–2050 (middle column) and 2080–2099 (right column). The rows represent the impact of CO_2 and NO_x emission, of CIC, of the non-CO_2 emissions and of all the emissions considered (Total impact). The shaded areas represent statistically significant changes at the 90 % level of confidence applying t-test.

ACPD
13, 3817–3858, 2013

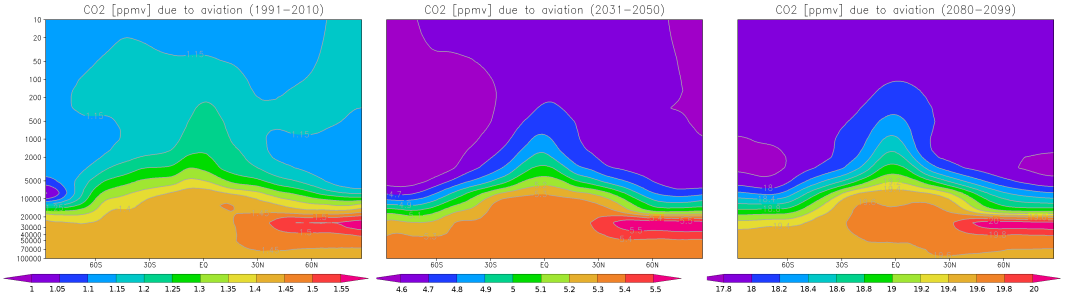

Fig. 10. Impact of aircraft CO_2 emissions on the zonally averaged CO_2 distribution for 1991–2010, 2031–2050 and 2080–2099 (ppmv). Note that the colorbar is different in each plot.

ACPD
13, 3817–3858, 2013

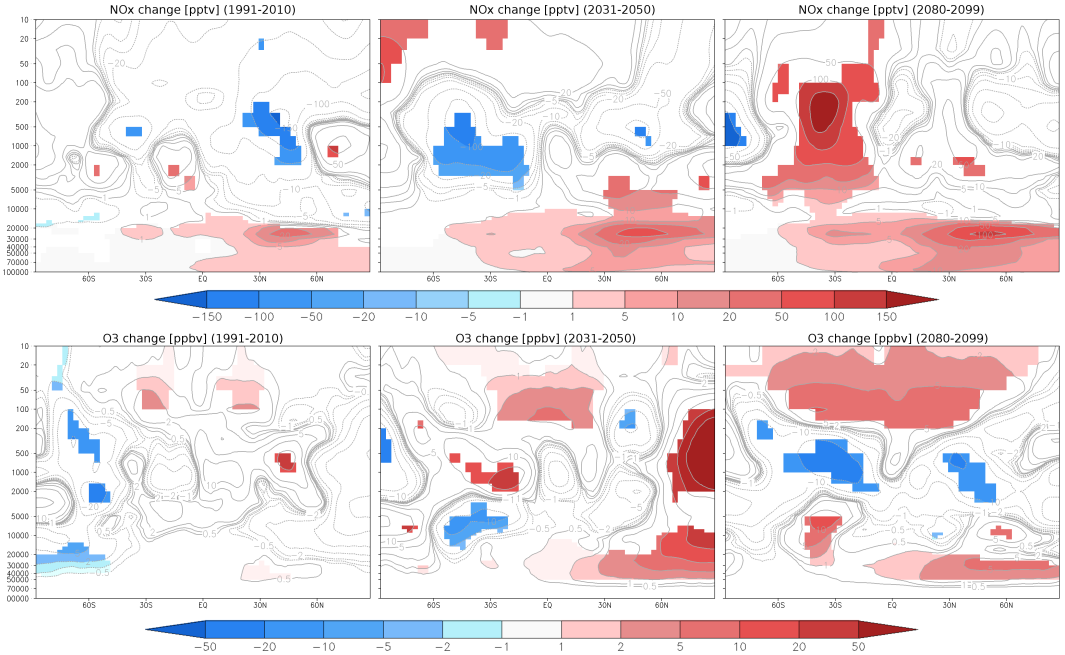

Fig. 11. Impact of aircraft NO_x emissions on the zonally averaged NO_x (pptv, upper row) and O_3 (ppbv, bottom row) distributions for 1991–2010, 2031–2050 and 2080–2099. The shaded areas show significant changes at the 90 % level of confidence.

ACPD
13, 3817–3858, 2013